

ULRR

On the local solute redistribution equation of macrosegregation, remelting and the formation of channel segregates

Item Type	Article
Authors	Vynnycky, Michael
Citation	International Journal of Heat and Mass Transfer 190, 122737
Publisher	Elsevier
Download date	2026-03-13 04:35:10
Item License	https://creativecommons.org/licenses/by-nc-sa/4.0/
Link to Item	https://doi.org/10.34961/researchrepository-ul.21673631



On the local solute redistribution equation of macrosegregation, remelting and the formation of channel segregates

M. Vynnycky^{a,b}

^a Mathematics Applications Consortium for Science and Industry (MACSI), Department of Mathematics and Statistics, University of Limerick, Limerick, V94 T9PX, Ireland

^b Division of Processes, Department of Materials Science and Engineering, KTH Royal Institute of Technology, Brinellvägen 23, Stockholm 100 44, Sweden



ARTICLE INFO

Article history:

Received 22 December 2021

Revised 17 February 2022

Accepted 24 February 2022

Available online 19 March 2022

Keywords:

Alloy solidification

Macrosegregation

Remelting

Channel segregates

ABSTRACT

In this paper, we reassess the local solute redistribution equation (LSRE) of macrosegregation which, since it first appeared in 1960s, has served as a cornerstone for understanding the composition variations that occur in the solidification of alloys. We highlight some anomalies in earlier literature, in particular as regards the prediction of remelting as a precursor to the formation of channel segregates (freckles, A-segregates and V-segregates) in casting processes. Also, we suggest extensions to the LSRE for situations where solute diffusion in the solid phase is not negligible, as well as when the mode of solidification is unconsolidated equiaxed dendritic, rather than columnar/consolidated equiaxed dendritic. In addition, the significance of the equation for latter-day numerical computations of macrosegregation is also discussed.

© 2022 The Author(s). Published by Elsevier Ltd.

This is an open access article under the CC BY license (<http://creativecommons.org/licenses/by/4.0/>)

1. Introduction

Macrosegregation refers to variations in composition that occur in alloy castings or ingots and which can range in scale from several millimetres to centimetres or even metres; it is a central problem, since it strongly influences the further workability of the cast products and their mechanical properties. As is already well-established [1], macrosegregation arises as a consequence of the nature of the solidification process for alloys, which involves the formation of a network of solid dendrites through which there is the slow flow of the remaining molten liquid, often termed the interdendritic melt, and the transport of alloying elements; the region where solid and liquid phase coexist is commonly referred to as a mush. In particular, as solidification occurs, if the solute is more soluble in liquid than in the solid phase, then it is rejected into the melt; as a consequence, there will be a non-uniform distribution of solute in the final solidified casting.

One of the cornerstones of the current understanding of macrosegregation during the solidification of alloys is the local solute redistribution equation (LSRE), first derived for a binary alloy by Flemings and Nereo [2]. In its original form, the LSRE was stated as

$$\frac{\partial g_L}{\partial C_L} = - \left(\frac{1 - \beta}{1 - k_0} \right) \left[1 + \frac{\mathbf{v}_L \cdot \nabla T}{\partial T / \partial t} \right] \frac{g_L}{C_L}, \quad (1)$$

where g_L is the liquid fraction, C_L is the solute concentration in the liquid phase, T is the temperature, \mathbf{v}_L is the interdendritic melt velocity, t is the time, β is the solidification shrinkage parameter and k_0 is the partition coefficient. This form has been cited on numerous occasions since [1,3–5], as has the purportedly equivalent form

$$\frac{\partial g_L}{\partial T} = - \left[\left(\frac{1 - \beta}{1 - k_0} \right) \frac{g_L}{C_L} \frac{\partial C_L}{\partial T} \right] \left(1 + \frac{\mathbf{v}_L \cdot \nabla T}{\partial T / \partial t} \right), \quad (2)$$

as given in [4,6,7]; this has also been extended for use in the case of multicomponent alloys [8,9]. Eq. (1) was subsequently the basis used for explaining how remelting can lead to the interdendritic flow instabilities that result in the formation of channel segregates [4], of which there are three main types: freckles, A-segregates and V-segregates. A schematic for the latter two, as they occur in ingot casting, is shown in Fig. 1, with freckles merely being considered as a special case of A-segregates when solidification occurs in the opposite direction to gravity. Moreover, while the mechanism for the formation of A-segregates is now reasonably well-established - being a consequence of the enrichment of the interdendritic melt with light solute elements, leading to a decrease in the local melt density and the onset of thermosolutal convection [10] - the mechanism for the formation of V-segregates, which are the only type of channel segregate to appear in continuous casting also [11–15], is less so [1,16]. Outside of the main metallurgical literature where channel segregates were first discussed, Fowler [17] and Worster [18] both refer to results in the book by Flemings [3], which fol-

E-mail address: michael.vynnycky@ul.ie

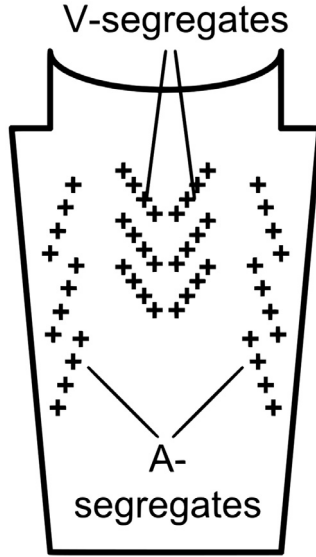


Fig. 1. A- and V-segregates in large ingots.

low directly from [2,4], in stating the condition for the formation of freckles as being

$$\frac{DT}{Dt} \equiv \frac{\partial T}{\partial t} + \mathbf{v}_L \cdot \nabla T > 0, \quad (3)$$

or alternatively

$$(\mathbf{v}_L - \mathbf{v}_{L,T}) \cdot \nabla T > 0, \quad (4)$$

where $\mathbf{v}_{L,T}$ denotes the isotherm velocity, which may also be interpreted as the solidification rate.

In this context, it is the purpose of this paper to investigate equation (1) more thoroughly; in so doing, a number of anomalies will be uncovered. Among these, it is found that although (3) and (4) both turn out to be correct, they cannot be extracted from the considerations in [3,4], which are in fact in themselves not entirely correct either. Moreover, although Fowler [17] and, subsequently, Emms and Fowler [19] obtained (3) and (4) via an alternative route to that in [4], their model contained assumptions that were not made in [2,4]. In addition, algebraic errors are found for the case of multicomponent alloys [8,9]. Although these may seem like petty details, there are at least two reasons to argue for the correct form of Eq. (1), both of which have to do with remelting as a necessary, although not sufficient, precursor to the formation of channel segregates. On the one hand, there remains substantial interest in the numerical computation of channel segregates in ingot casting, although there is still significant doubt as to whether they are being computed correctly [20–22]. A more appropriate form of Eq. (1) could provide a diagnostic to verify whether such computations are indeed correct; however, Eq. (1) does not provide such a diagnostic, not least because such simulations do not compute $\partial g_L / \partial C_L$ explicitly. Indeed, it is not obvious that such simulations make use of Eq. (1) or the correct form of it at all, and one of the observations here will be that the correct form of Eq. (1) does indeed arise from the volume-averaged approach for the conservation equations that is often used for such simulations. Secondly, there is the issue of how Eq. (1) should be applied in the case of the only type of channel segregate that occurs in continuous casting processes, i.e. V-segregates; this would be timely, as there is still no detailed theoretical model for the formation of V-segregates, neither for continuous casting nor ingot casting, in contrast to the detailed models that already exist for the formation of freckles [17,19,23,24] and A-segregates in ingot casting [6].

The layout of this paper is as follows. In Section 2, the governing equations relevant to an ingot casting situation for a binary alloy are formulated; these pertain to the mushy zone, wherein solid and liquid phases are known to coexist and which is where the flow instabilities that give rise to channel segregates occur. In Sections 3 and 4, the governing equations are analyzed in the context of remelting and whether the mode of solidification is columnar/consolidated equiaxed dendritic or unconsolidated equiaxed dendritic, respectively. In Sections 5 and 6, the significance of the analysis is discussed in the context of continuous casting, and conclusions are drawn in Section 7.

2. Governing equations

Here, the general volume-averaged conservation equations for columnar/consolidated equiaxed dendritic solidification discussed in [25], supplemented by the back-diffusion treatment proposed in [26], is adopted; this formulation was recently used in [27–29]. The assumptions are that: solidification occurs with little undercooling; solute equilibrium is maintained at the liquid-solid interface throughout solidification; solute diffusion in the liquid is complete between the small dendritic channels; solid density is constant; no pores form. These assumptions were also made by Flemings and co-workers [2,4,8]; however, their assumption concerning solute diffusion in the solid is relaxed, allowing it to be arbitrary, rather than negligible.

The total mass balance over solid and liquid phases in the mush, derived from summing the phase conservation equations, is given by

$$\frac{\partial \rho}{\partial t} + \nabla \cdot (\rho_L g_L \mathbf{v}_L) = 0, \quad (5)$$

where ρ_L is the density of the liquid phase, g_L is the liquid fraction and with the mass-averaged velocity consisting only of the liquid phase velocity, \mathbf{v}_L , since the solid does not move and its velocity is therefore zero. Also, ρ is the mixture density and is written as

$$\rho = g_L \rho_L + (1 - g_L) \rho_S, \quad (6)$$

where ρ_S is the density of the solid phase; typically for metal alloys, $\rho_S > \rho_L$. For ρ_L , an often-used form is

$$\rho_L = \rho_{ref} (1 - \alpha_T (T - T_{ref}) + \alpha_C (C - C_{ref})), \quad (7)$$

where $\alpha_T, \alpha_C > 0$, with ρ_{ref}, T_{ref} and C_{ref} as a reference density, temperature and concentration, respectively; ρ_{ref}, T_{ref} and C_{ref} are all constants.

The momentum balance for the liquid phase is given in simplified form by

$$\mu g_L \mathbf{v}_L = \kappa \cdot (-\nabla p + \rho_L \mathbf{g}) \quad (8)$$

where μ is the dynamic viscosity of the liquid phase, p is the pressure, \mathbf{g} is the acceleration due to gravity and κ is the permeability tensor for the mushy region. Typically, κ is taken to be of the isotropic form $\kappa \mathbf{I}$, where \mathbf{I} is the identity matrix and κ is a function of the liquid fraction, given often by the Carman-Kozeny relation as

$$\kappa(g_L) = \frac{\kappa_0 g_L^3}{(1 - g_L)^2}, \quad (9)$$

where κ_0 is given in terms of the primary or secondary dendrite arm spacings.

The conservation of energy is given by

$$\begin{aligned} & \frac{\partial}{\partial t} (\{\rho_L c_{p,L} g_L + \rho_S c_{p,S} (1 - g_L)\} T) + \nabla \cdot (\rho_L c_{p,L} g_L \mathbf{v}_L T) \\ & = \nabla \cdot (k \nabla T) - \Delta H_f \frac{\partial}{\partial t} (\rho_L g_L), \end{aligned} \quad (10)$$

where $c_{p,L}$ and $c_{p,S}$ denote, respectively, the specific heat capacities of the liquid and solid phases, ΔH_f is the latent heat of fusion and k is the mixture thermal conductivity, given by

$$k = g_L k_L + (1 - g_L) k_S, \quad (11)$$

where k_L and k_S denote the thermal conductivities of the melt and solid phases, respectively.

The equation for the conservation of solute, taken over solid and liquid phases, is given by

$$\frac{\partial}{\partial t} (\rho C) + \nabla \cdot (\rho_L C_L g_L \mathbf{v}_L) = 0, \quad (12)$$

where the form for the mixture concentration, C , depends on the assumption made regarding solute transport at the microscale. The two extremes are the lever rule and the Scheil equation, where

$$\rho C = g_L \rho_L C_L + \begin{cases} \rho_S (1 - g_L) C_S, & \text{lever rule} \\ \rho_S \int_0^{1-g_L} C_S dg'_L, & \text{Scheil equation} \end{cases}, \quad (13)$$

with C_L and C_S as the concentrations of the solute in the liquid and solid phases, respectively, which are related by

$$C_S = k_0 C_L, \quad (14)$$

where k_0 is the partition coefficient, with $0 < k_0 < 1$; moreover, the lever rule assumes thermodynamic equilibrium between the phases, whereas the Scheil equation assumes no solute diffusion in the solid and perfect mixing in the liquid. For the purposes of generalization, it is possible to introduce a parameter γ , where $0 \leq \gamma \leq 1$, that allows for a back-diffusion treatment, i.e. partial solute diffusion into the solid, that lies between the limits of zero back diffusion ($\gamma = 0$, the Scheil assumption) and complete back diffusion ($\gamma = 1$, the lever rule); as indicated by Swaminathan and Voller [26], this treatment of back diffusion is equivalent to using the Clyne and Kurz correction [30] of the well-known back diffusion model of Brody and Flemings [31]. Following [26] in first setting

$$\int_0^{1-g_L} \frac{\partial C_S}{\partial t} dg'_L = \gamma (1 - g_L) k_0 \frac{\partial C_L}{\partial t}, \quad (15)$$

Eq. (12) becomes

$$\rho_L \frac{\partial}{\partial t} (g_L C_L) - k_0 \rho_S C_L \frac{\partial g_L}{\partial t} + \rho_S \gamma (1 - g_L) k_0 \frac{\partial C_L}{\partial t} + \nabla \cdot (\rho_L C_L g_L \mathbf{v}_L) = 0; \quad (16)$$

furthermore, Eq. (13) can now be generalized for $0 \leq \gamma \leq 1$ to give

$$\rho C = g_L \rho_L C_L + \rho_S \int_0^{1-g_L} \left(C_S + \gamma g'_L \frac{dC_S}{dg'_L} \right) dg'_L. \quad (17)$$

It should also be noted that, if remelting occurs, the above approach will only be valid when $\gamma = 1$, i.e. when there is complete diffusion in the solid. In this case, it can be assumed that the composition of the remelting solid is equal to the current solid composition and no special care needs to be taken to account for remelting, since the solid concentration will equal the partition coefficient multiplied by the interface liquid concentration. When $\gamma \neq 1$, the presence of a microscopic concentration profile in the solid requires special remelting models [23,32–34]. In this case, the entire average solid concentration history needs to be tracked, and the correct liquid fraction is determined by backward time interpolation to find the liquid fraction and the average solid concentration. However, as we are considering the conditions necessary for remelting to occur, rather than what happens after it occurs, we will not need to concern ourselves with these details here.

Assuming local thermodynamic equilibrium in the mushy region, the liquidus curve in the phase diagram for the alloy under consideration is given by

$$T = f(C_L) \quad \text{for } 0 \leq g_L \leq 1, \quad (18)$$

with a common approximation for $f(C_L)$ being

$$f(C_L) = T_m - m C_L, \quad (19)$$

where T_m is the melting point of the solvent element and with $m > 0$; we will not explicitly assume this form here, although we will suppose that $f'(C_L) < 0$, where the prime denotes differentiation with respect to C_L .

In what follows, we will mainly focus on Eqs. (5), (16) and (18), making little use of (8) and (10). Also, we omit any detailed discussion of the initial and boundary conditions for Eqs. (5), (8), (10) and (16), as these will not be of relevance here.

3. Analysis for columnar dendritic solidification

A commonly used approach is to adopt the Boussinesq approximation, meaning that the full form for ρ_L , Eq. (7), is used only in Eq. (8), and that ρ_L is taken to be constant everywhere else that it appears in Eqs. (5), (10) and (16). Moreover, we can now note that (5) and (16) are identical to Eqs. (5) and (7), respectively, in [2], meaning that we can directly link it, and the results that follow from it, to any conclusions that follow from the volume-averaged approach that was first established much later [25]. By eliminating $\nabla \cdot \mathbf{v}_L$, Eqs. (5) and (16) can now be combined to give

$$\left(1 + \frac{\gamma}{g_L} \left(\frac{1 - g_L}{1 - \beta} \right) k_0 \right) \frac{\partial C_L}{\partial t} = - \left(\frac{1 - k_0}{1 - \beta} \right) \frac{C_L}{g_L} \frac{\partial g_L}{\partial t} - \mathbf{v}_L \cdot \nabla C_L, \quad (20)$$

where $\beta = (\rho_S - \rho_L) / \rho_S$, where now $\rho_L = \rho_{ref}$; with $\gamma = 0$, we have the form given in [2],

$$\frac{\partial C_L}{\partial t} = - \left(\frac{1 - k_0}{1 - \beta} \right) \frac{C_L}{g_L} \frac{\partial g_L}{\partial t} - \mathbf{v}_L \cdot \nabla C_L, \quad (21)$$

Next, in Section 3.1, we first revisit the argument used in [2] to obtain the LSRE. After that, in Section 3.2, we consider how the LSRE is used to inform on remelting.

3.1. LSRE

To reach Eq. (1) from Eq. (21) in [2] required the following steps.

1. $\mathbf{v}_L \cdot \nabla C_L$ was replaced by $\frac{\mathbf{v}_L \cdot \nabla T}{\partial T / \partial t} \frac{\partial C_L}{\partial t}$, by considering what happens at an isotherm. However, at an isotherm, while it is certainly true that

$$\frac{\partial T}{\partial t} + \mathbf{v}_{L,T} \cdot \nabla T = 0, \quad \frac{\partial C_L}{\partial t} + \mathbf{v}_{L,T} \cdot \nabla C_L = 0, \quad (22)$$

where $\mathbf{v}_{L,T}$ is the velocity of an isotherm, and thence that

$$\frac{\mathbf{v}_{L,T} \cdot \nabla C_L}{\partial C_L / \partial t} = -1 = \frac{\mathbf{v}_{L,T} \cdot \nabla T}{\partial T / \partial t}, \quad (23)$$

it is not, in general, the case that $\mathbf{v}_{L,T} = \mathbf{v}_L$. Indeed, if this were the case, Eq. (4) would never be satisfied, meaning that freckles would never form.

2. Having then arrived at

$$\frac{\partial g_L}{\partial t} = - \left(\frac{1 - \beta}{1 - k_0} \right) \left(1 + \frac{\mathbf{v}_L \cdot \nabla T}{\partial T / \partial t} \right) \frac{g_L}{C_L} \frac{\partial C_L}{\partial t}, \quad (24)$$

both sides are divided by $\frac{\partial C_L}{\partial t}$ to obtain Eq. (1); however, this can only be true if $g_L = g_L(t)$ and $C_L = C_L(t)$, so that

$$\frac{dg_L}{dt} / \frac{dC_L}{dt} = \frac{dg_L}{dC_L}.$$

However, a stronger argument is the following. On using Eq. (18), we have that

$$\frac{\partial T}{\partial t} = f'(C_L) \frac{\partial C_L}{\partial t}, \quad \mathbf{v}_L \cdot \nabla T = f'(C_L) \mathbf{v}_L \cdot \nabla C_L, \quad (25)$$

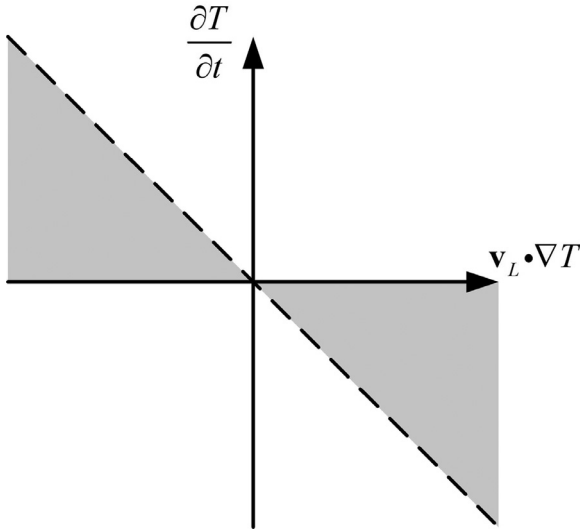


Fig. 2. The criterion for remelting in terms of $\frac{\partial T}{\partial t}$ and $\mathbf{v}_L \cdot \nabla T$. The considerations in [4] for $\gamma = 0$ indicate that $(\frac{\partial T}{\partial t} \cdot \mathbf{v}_L \cdot \nabla T)$ combinations in the shaded regions will lead to remelting, whereas the actual result, from criterion (34), is that it should occur when $\frac{\partial T}{\partial t} > -\mathbf{v}_L \cdot \nabla T$.

whence

$$\mathbf{v}_L \cdot \nabla C_L = \frac{\mathbf{v}_L \cdot \nabla T}{\partial T / \partial t} \frac{\partial C_L}{\partial t}, \quad (26)$$

so that Eq. (24) gives

$$\left(\frac{1-k_0}{1-\beta}\right) C_L \frac{\partial g_L}{\partial t} = -g_L \left(1 + \frac{\mathbf{v}_L \cdot \nabla T}{\partial T / \partial t}\right) \frac{\partial C_L}{\partial t}, \quad (27)$$

which can be simplified to

$$\left(\frac{1-k_0}{1-\beta}\right) C_L \frac{\partial g_L}{\partial t} = -\frac{g_L}{f'(C_L)} \frac{DT}{Dt}. \quad (28)$$

Moreover, it is straightforward to extend this to the case when $\gamma \neq 0$ to obtain

$$\left(\frac{1-k_0}{1-\beta}\right) C_L f'(C_L) \frac{\partial g_L}{\partial t} = -\left\{g_L \frac{DT}{Dt} + \gamma \left(\frac{1-g_L}{1-\beta}\right) k_0 \frac{\partial T}{\partial t}\right\}. \quad (29)$$

3.2. Remelting

In addition, Mehrabian et al. [4] suggest multiplying equation (1) by $\partial C_L / \partial t$ to obtain Eq. (2). With the quantity inside the square brackets of Eq. (2) supposedly negative regardless of the value of k_0 , the discussion in [4] hinges on the value of $1 + \mathbf{v}_L \cdot \nabla T / (\partial T / \partial t)$. In particular, if

$$\mathbf{v}_L \cdot \nabla T / (\partial T / \partial t) < -1, \quad (30)$$

remelting is said to occur, since it will mean that $\partial g_L / \partial t < 0$; see also [6,7]. In fact, this argument would lead to having to consider the cases

$$\frac{\partial T}{\partial t} + \mathbf{v}_L \cdot \nabla T > 0, \quad \frac{\partial T}{\partial t} < 0 \quad (31)$$

and

$$\frac{\partial T}{\partial t} + \mathbf{v}_L \cdot \nabla T < 0, \quad \frac{\partial T}{\partial t} > 0, \quad (32)$$

separately, as shown in Fig. 2.

However, the discussion becomes much simpler if we use equation (29). For remelting at any point, we must have

$$\partial g_L / \partial t > 0 \quad (33)$$

at that point, i.e. the liquid fraction locally increases with time, and since $f'(C_L) < 0$, $k_0 < 1$, $\beta < 1$, we obtain, from Eq. (29),

$$g_L \left(\frac{\partial T}{\partial t} + \mathbf{v}_L \cdot \nabla T\right) + \gamma \left(\frac{1-g_L}{1-\beta}\right) k_0 \frac{\partial T}{\partial t} > 0, \quad (34)$$

which reduces to (3) if $\gamma = 0$, which is the form cited in [17,19]; note, however, that (3) does not correspond to (30). Observe also that neither Eq. (3) nor (34) indicate any particular position in the mushy zone where remelting should first occur. On the other hand, the detailed models of [17,19,24] give that criterion (3) should be satisfied at the liquidus isotherm; we will return to this point when considering unconsolidated equiaxed dendritic solidification in Section 4. Furthermore, it should be noted that in these models, as well others in the non-metallurgical literature [18,35], it is effectively the lever rule that is being assumed at the microscale, i.e. $\gamma = 1$, and it is therefore perhaps, at first sight, surprising that (3) was obtained at all. The explanation comes from the fact that k_0 was set to zero in these models, in which case (34) reduces to (3).

Now, for any isotherm, we can use Eqs. (22) and (29) to obtain

$$\left(\frac{1-k_0}{1-\beta}\right) C_L \frac{\partial g_L}{\partial t} = -\frac{g_L}{f'(C_L)} \left\{\mathbf{v}_L - \left(1 + \frac{\gamma}{g_L} \left(\frac{1-g_L}{1-\beta}\right) k_0\right) \mathbf{v}_{L,T}\right\} \cdot \nabla T, \quad (35)$$

so that $\partial g_L / \partial t > 0$ implies that

$$\left\{\mathbf{v}_L - \left(1 + \frac{\gamma}{g_L} \left(\frac{1-g_L}{1-\beta}\right) k_0\right) \mathbf{v}_{L,T}\right\} \cdot \nabla T > 0, \quad (36)$$

which is the generalization of Eq. (4).

4. Analysis for unconsolidated equiaxed dendritic solidification

The discussion to date has concerned columnar or consolidated equiaxed dendritic solidification, for which the solid phase velocity is zero; it is thus of interest to understand how the LSRE will differ in the unconsolidated equiaxed zone of a metal casting, which consists of free-floating dendrites and where the solid phase velocity, \mathbf{v}_S , is not zero. One of the simplest approaches is to take $\mathbf{v}_S = \mathbf{v}_L$ [36–38]; this is often referred to as the mushy fluid model, and is applicable to amorphous materials, e.g. waxes and glasses, and in a limited sense, the unconsolidated equiaxed zone of a metal casting. In the mushy fluid, the solid is usually assumed to be fully dispersed within the liquid and moving with the same velocity, with the lever rule applying at the microscale, i.e. $\gamma = 1$; here, however, we consider the general case, i.e. $0 \leq \gamma \leq 1$.

Now, Eqs. (5) and (16) are replaced by

$$\frac{\partial \rho}{\partial t} + \nabla \cdot (\rho_L g_L \mathbf{v}_L + \rho_S (1 - g_L) \mathbf{v}_S) = 0, \quad (37)$$

$$\begin{aligned} \frac{\partial}{\partial t} (\rho_L g_L C_L) - \rho_S k_0 C_L \frac{\partial g_L}{\partial t} + \gamma \rho_S (1 - g_L) k_0 \frac{\partial C_L}{\partial t} + \nabla \cdot (\rho_L g_L C_L \mathbf{v}_L) \\ + k_0 \rho_S [-C_L \mathbf{v}_S \cdot \nabla g_L + \gamma (1 - g_L) \{\mathbf{v}_S \cdot \nabla C_L + C_L \nabla \cdot \mathbf{v}_S\}] = 0, \end{aligned} \quad (38)$$

respectively. With $\mathbf{v}_S = \mathbf{v}_L$, we have

$$-\beta \frac{\partial g_L}{\partial t} + \nabla \cdot \{(1 - \beta g_L) \mathbf{v}_L\} = 0, \quad (39)$$

$$(1 - \beta) \frac{\partial}{\partial t} (g_L C_L) - k_0 C_L \frac{\partial g_L}{\partial t} + \gamma (1 - g_L) k_0 \frac{\partial C_L}{\partial t} +$$

$$(1 - \beta) \nabla \cdot (g_L C_L \mathbf{v}_L) + k_0 [-C_L \mathbf{v}_L \cdot \nabla g_L + \gamma (1 - g_L) \nabla \cdot (C_L \mathbf{v}_L)] = 0. \quad (40)$$

As in Section 3, the idea is to eliminate the $\nabla \cdot \mathbf{v}_L$ term between Eqs. (39) and (40). Expanding these out, we obtain

$$\beta \frac{\partial g_L}{\partial t} + \beta \mathbf{v}_L \cdot \nabla g_L = (1 - \beta g_L) \nabla \cdot \mathbf{v}_L, \quad (41)$$

$$(1 - \beta) \frac{\partial}{\partial t} (g_L C_L) - k_0 C_L \frac{\partial g_L}{\partial t} + \gamma (1 - g_L) k_0 \frac{\partial C_L}{\partial t} + (1 - \beta - k_0) C_L \mathbf{v}_L \cdot \nabla g_L + \{(1 - \beta) g_L + k_0 \gamma (1 - g_L)\} \mathbf{v}_L \cdot \nabla C_L = -\{(1 - \beta) g_L + k_0 \gamma (1 - g_L)\} C_L \nabla \cdot \mathbf{v}_L, \quad (42)$$

respectively, and eliminate $\nabla \cdot \mathbf{v}_L$ to arrive at

$$\frac{\partial}{\partial t} (\{(1 - \beta - k_0) g_L + k_0\} C_L) + (\gamma - 1) (1 - g_L) k_0 \frac{\partial C_L}{\partial t} + \mathbf{v}_L \cdot \nabla (\{(1 - \beta - k_0) g_L + k_0\} C_L) + k_0 (\gamma - 1) (1 - g_L) \mathbf{v}_L \cdot \nabla C_L = -\beta \left\{ \frac{(1 - \beta - \gamma k_0) g_L + \gamma k_0}{-\beta g_L + 1} \right\} C_L \left[\frac{\partial g_L}{\partial t} + \mathbf{v}_L \cdot \nabla g_L \right]; \quad (43)$$

expanding out still further results in

$$R[1 - k_0 + (\gamma - 1)(1 - R)k_0(1 - g_L)] C_L \frac{Dg_L}{Dt} = -[(1 - R)g_L + R]\{g_L + \gamma k_0 R(1 - g_L)\} \frac{DC_L}{Dt}, \quad (44)$$

where $R = 1/(1 - \beta)$. Now, although (44) is a non-linear partial differential equation, it can nevertheless still be integrated. Rewriting it as

$$\frac{[1 - k_0 - (\gamma - 1)(1 - R)k_0(1 - g_L)] Dg_L}{(1 - \beta g_L)\{(1 - \beta)g_L + \gamma k_0(1 - g_L)\} Dt} = -\frac{1}{C_L} \frac{DC_L}{Dt}, \quad (45)$$

we can then obtain

$$\frac{D}{Dt} \left(\ln \left(\frac{[(1 - \gamma k_0 R)g_L + \gamma k_0 R]^\mu}{(1 - R)g_L + R} \right) + \ln C_L \right) = 0, \quad (46)$$

where

$$\mu = \frac{(1 - k_0)(1 - \beta - \gamma k_0) + k_0(\gamma - 1)\beta}{(1 - \gamma k_0)(1 - \beta - \gamma k_0)}. \quad (47)$$

Assuming, as is reasonable, that at $t = 0$ there is only melt having solute composition C_0 , we have

$$C_L = C_0, \quad g_L = 1 \quad \text{at } t = 0; \quad (48)$$

we can then integrate Eq. (46) to obtain

$$C_L = \frac{C_0(1 - \beta g_L)}{[(1 - \beta - \gamma k_0)g_L + \gamma k_0]^\mu}. \quad (49)$$

When $\beta = 0$, we have

$$C_L = \frac{C_0}{[(1 - \gamma k_0)g_L + \gamma k_0]^\mu}, \quad \mu = \frac{1 - k_0}{1 - \gamma k_0}, \quad (50)$$

with $\gamma = 0$ and 1 giving the usual Scheil equation and lever rule, respectively; nevertheless, with $\beta \neq 0$, Eq. (49) constitutes a new result. Moreover, it identifies that even when the velocities of the phases are non-zero, there is a closed-form expression that relates C_L and g_L ; thence, on using Eq. (18), we can relate T directly to C_L and g_L also.

We may now also consider the significance of Eq. (49), as regards the possibility of remelting. Differentiating (49) with respect to t , we have

$$\frac{\partial C_L}{\partial t} = \frac{C_0 h(g_L)}{(1 - \gamma k_0)[(1 - \gamma k_0 R)g_L + \gamma k_0 R]^{\mu+1}} \frac{\partial g_L}{\partial t}, \quad (51)$$

where

$$h(g_L) = (1 - R)[(1 - \gamma k_0 R)g_L + \gamma k_0 R](1 - \gamma k_0) - [(1 - k_0)(1 - \gamma k_0 R) - k_0(\gamma - 1)(1 - R)]((1 - R)g_L + R); \quad (52)$$

so, we need to consider the sign of $h(g_L)$. Rewriting Eq. (52) as

$$h(g_L) = A g_L + B, \quad (53)$$

where

$$A = k_0 R(1 - \gamma)(1 - R)(1 - \gamma k_0), \quad (54)$$

$$B = R\{(1 - R)k_0[-\gamma^2 k_0 + 2\gamma - 1] - (1 - k_0)(1 - \gamma k_0 R)\}, \quad (55)$$

it is evident that $A \leq 0$. As for B , we rewrite this as

$$B = R\bar{B}(\gamma),$$

where

$$\bar{B}(\gamma) = (R - 1)k_0^2 \gamma^2 + (2 - R(k_0 + 1))k_0 \gamma + (Rk_0 - 1).$$

It is clear that $\bar{B}(0) = k_0 R - 1$ and $\bar{B}(1) = -(1 - k_0)^2$. It is usually the case that $1 < R < 1/k_0$; hence, $\bar{B}(0) < 0$, $\bar{B}(1) < 0$. Also, in view of the form of \bar{B} , i.e. the coefficient in front of the γ^2 term is positive, it cannot have a local maximum. Therefore, there is no value of γ for $0 \leq \gamma \leq 1$ such that $\bar{B}(\gamma) > 0$; hence, $\bar{B}(\gamma) < 0$ for $0 \leq \gamma \leq 1$ and thus $h(g_L) < 0$ for $0 \leq g_L \leq 1$. Now, from Eqs. (18) and (51), we have

$$(1 - \beta) \frac{\partial g_L}{\partial t} = \frac{(1 - \gamma k_0)[(1 - \beta - \gamma k_0)g_L + \gamma k_0]^{\mu+1}}{C_0 h(g_L) f'(C_L)} \frac{\partial T}{\partial t}. \quad (56)$$

So, for $\partial g_L / \partial t > 0$, we would need $\partial T / \partial t > 0$.

Returning to the detailed models in [17,19,24], recall that these assumed columnar dendritic solidification and found that channelling starts where $g_L = 1$. This would be self-consistent if this were the only solidification mode. In general, however, during a casting process, both columnar/consolidated equiaxed and unconsolidated equiaxed dendritic solidification occur; this happens in regions in which the solid fraction, $g_S (= 1 - g_L)$, is above and below, respectively, a critical value known as the packing fraction, $g_{S,p}$; whilst its value varies from system to system, an upper value is typically around 0.3 [39], corresponding to $g_L \approx 0.7$. Thus, if remelting were to first occur in the unconsolidated equiaxed region of a mushy zone, the condition for remelting would no longer be (34), but just $\partial T / \partial t > 0$.

5. Significance for V-segregates in the continuous casting of steel

In the continuous casting of steel, V-segregates are known to form about the axis of symmetry, as shown in Fig. 3, although the mechanism of formation remains unclear [11–14]; this is discussed further in Section 6.2. Indeed, perhaps the only thing which can be said with any degree of clarity, based on experimental observations [11,13], is that V-segregates are more likely to manifest when there is an equiaxed zone in the centre of the casting. Moreover, V-segregates must clearly form in the part of the mushy region that is close to the point of complete solidification. In this region, since the solid fraction is very high, it is more likely that equiaxed crystals that are there have consolidated after settling, rather than being of the free-moving and unconsolidated type that one might expect in the mushy zone higher up the caster, where the solid fraction is much lower.

Although we will not provide a model for V-segregate formation here, it is nevertheless possible to discuss some of the features that such a model would need to have. First of all, and perhaps rather paradoxically, we note that continuous casting is typically considered to be a steady state process, in the sense that

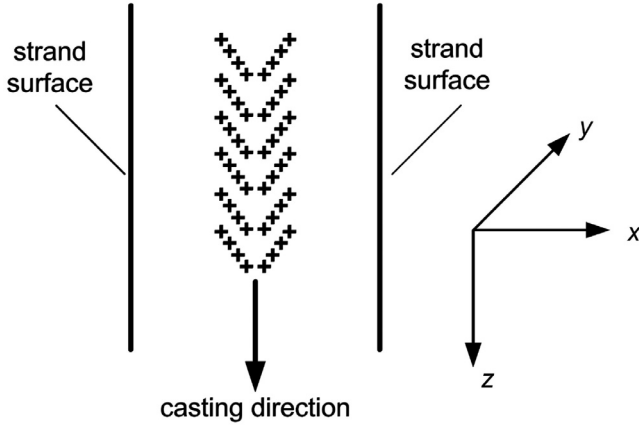


Fig. 3. Schematic diagram of V-segregates in continuous casting. Length cutting of the solidified strand.

the solidified strand is withdrawn at a constant casting speed; on the other hand, the appearance of V-segregates suggests such that it is not steady state, since it is clear that the concentration profiles that are frozen into the final solidified sample must have varied with time. Consequently, this phenomenon cannot be captured with a steady state model, as can other types of segregation that occur in continuous casting, e.g. centreline segregation or inverse segregation. Thus, what is required is a transient model that takes into account constant casting speed. In what follows, we consider how Eqs. (37) and (38) should be developed to do this. For simplicity, we consider here only the equations for a binary alloy, even though in practice V-segregates can be found in multicomponent steels [13,14]; nevertheless, we give the corresponding result for a multicomponent alloy at the end of appendix A.

With $\mathbf{v}_S = (0, 0, V_{\text{cast}})$, where V_{cast} denotes the casting speed, Eqs. (37) and (38) become

$$-\beta \frac{\partial g_L}{\partial t} + (1 - \beta) \nabla \cdot (g_L \mathbf{v}_L) - V_{\text{cast}} \frac{\partial g_L}{\partial z} = 0, \quad (57)$$

$$(1 - \beta) \frac{\partial}{\partial t} (g_L C_L) - k_0 C_L \frac{\partial g_L}{\partial t} + \gamma (1 - g_L) k_0 \frac{\partial C_L}{\partial t}$$

$$+ (1 - \beta) \nabla \cdot (g_L C_L \mathbf{v}_L) + k_0 V_{\text{cast}} \left[\gamma (1 - g_L) \frac{\partial C_L}{\partial z} - C_L \frac{\partial g_L}{\partial z} \right] = 0, \quad (58)$$

respectively; here, z denotes the casting direction. Eliminating $\nabla \cdot (g_L \mathbf{v}_L)$ between equations (57) and (58), we obtain

$$(1 - k_0) C_L f'(C_L) \frac{\mathcal{D}g_L}{\mathcal{D}t} = -(1 - \beta) g_L \frac{\mathcal{D}T}{\mathcal{D}t} - \gamma (1 - g_L) k_0 \frac{\mathcal{D}T}{\mathcal{D}t}, \quad (59)$$

where

$$\frac{\mathcal{D}}{\mathcal{D}t} \equiv \frac{\partial}{\partial t} + V_{\text{cast}} \frac{\partial}{\partial z}.$$

Then, for remelting, we require $\partial g_L / \partial t > 0$, which leads to

$$g_L \frac{\mathcal{D}T}{\mathcal{D}t} + \gamma \left(\frac{1 - g_L}{1 - \beta} \right) k_0 \frac{\mathcal{D}T}{\mathcal{D}t} > - \left(\frac{1 - k_0}{1 - \beta} \right) C_L f'(C_L) V_{\text{cast}} \frac{\partial g_L}{\partial z}, \quad (60)$$

and reduces to (34) when $V_{\text{cast}} = 0$.

6. Discussion

We now discuss the above results in the contexts of the numerical simulation of alloy solidification in general, and the formation of V-segregates in continuous casting in particular.

6.1. Numerical simulation of alloy solidification

It is by now well-established that the use of computational fluid dynamics (CFD) in order to simulate alloy solidification, and macrosegregation profiles in particular, is fraught with difficulties [40–43]. Typically, numerical dispersion and diffusion is present in the simulated macrosegregation profiles reported in the literature, hindering the interpretation of CFD results; in particular, authors have found that using an unstructured mesh eliminates the numerical dispersion that is present when using a structured mesh, but it introduces numerical diffusion. On the other hand, using a refined structured mesh alleviates problems with numerical oscillations, but has been found to increase the computation time dramatically [44]. In the case when channel segregates form, the issue is further exacerbated, and there is still ongoing doubt as to whether, for example, A-segregates in ingot casting are being computed correctly [20–22], as regards mesh independence; this refers to their width, their length and the spacing between them. In this context, the contribution of this paper is to derive equations that can provide a consistency check on whether a numerical code is computing the intended equations correctly. To see how, recall equations (29) and (59), which are for the ingot and continuous casting, respectively, of a binary alloy; their counterparts for a multicomponent alloy are given by equations (A7) and (A11), respectively. In particular, they contain quantities that would be computed in the course of a numerical simulation of the solidification of an alloy, i.e. C_L , g_L , T and \mathbf{v}_L ; thus, at each time step and each point in the physical space, one can check that these equations are indeed being satisfied. As a corollary to this, one is able to obtain the conditions for remelting, given by (34)/(A8) and (60)/(A12), which can be considered as necessary, although not sufficient, conditions for the formation of channel segregates. Also, criteria (34)/(A8) can be considered as complements to existing approaches based on local Rayleigh number for predicting the onset of freckles and A-segregates [45–48]; moreover, these criteria may help to resolve where in the mushy zone the channel actually nucleates [10]. As for V-segregates, there is as yet no agreement on the mechanisms that cause them in ingot casting, although (34)/(A8) will be of relevance there also. Moreover, some of the candidates for such a mechanism are similar to those in continuous casting, and are discussed in detail next.

6.2. V-segregates in continuous casting

In continuous casting, early work by Tomono et al. [11] observed that V-segregates only occurred in the equiaxed grain zone of a continuously cast billet; this prompted the suggestion that the enriched liquid between the equiaxed crystals is sucked in and flows downwards and that, with the forcible movement of the piling equiaxed crystals to the billet centre, the enriched liquid accumulates along some planes, leading to the pattern seen in Fig. 3. Later on, based on experimental observation, Abbott et al. [13] proposed that V-segregation is induced by hot tearing and erosion of the solid by flowing segregated liquid. More recently, Ma and Li [14] attributed V-segregation to fissures in the equiaxed dendritic network torn by solidification contraction. Indeed, all of these mirror the mechanisms for the formation of V-segregates also suggested for ingot casting [1,3], although there is as yet no detailed mathematical model for this. Lastly, however, one may mention the recent modelling work by Guan et al. [15], which does appear to reproduce a V-segregate pattern, although it is not clear if this is merely a numerical artefact, since the authors did not consider any of three candidate mechanisms mentioned above; thus, since the computations in [15] were for a binary alloy, one would need to confirm that criterion (60) really is being satisfied. Nevertheless, given that any theoretical investigation of V-segregate formation will ultimately require numerical computation, it is clear that the

remelting criteria presented in this paper will have a role to play in determining the fidelity of such simulations.

7. Conclusions

In this paper, we have reassessed the local solute redistribution equation (LSRE) of macrosegregation which, since it first appeared in 1960s, has served as a cornerstone for understanding the composition variations that occur in the solidification of alloys. We have highlighted some anomalies in earlier literature, in particular as regards the prediction of remelting as a precursor to the formation of channel segregates (freckles, A-segregates and V-segregates) in casting processes. Extensions to the LSRE were suggested for situations where solute diffusion in the solid phase is not negligible, as well as when the mode of solidification is unconsolidated equiaxed dendritic, rather than columnar or consolidated equiaxed dendritic, and for continuous casting, where the solid phase is transported at constant speed in the casting direction.

Declaration of Competing Interest

The author declares that he has no known competing financial interests or personal relationships that could have appeared to influence the work reported in this paper.

CRediT authorship contribution statement

M. Vynnycky: Conceptualization, Methodology, Formal analysis, Writing – original draft, Writing – review & editing.

Acknowledgement

The author acknowledges useful discussions with Dr. B. Rogberg.

Appendix A. multicomponent alloys undergoing columnar/consolidated equiaxed dendritic solidification

For the case of $(n + 1)$ -component alloys undergoing columnar/consolidated equiaxed dendritic solidification, we retain Eq. (5), whilst Eq. (16) is replaced by, for $j = 1, \dots, n$,

$$\rho_L \frac{\partial}{\partial t} \left(g_L C_L^{(j)} \right) - k_0 \rho_S C_L^{(j)} \frac{\partial g_L}{\partial t} + \rho_S \gamma^{(j)} (1 - g_L) k_0^{(j)} \frac{\partial C_L^{(j)}}{\partial t} + \nabla \cdot \left(\rho_L C_L^{(j)} g_L \mathbf{v}_L \right) = 0, \quad (\text{A1})$$

and (18) is replaced by

$$T = f(C_L^{(1)}, C_L^{(2)}, \dots, C_L^{(n)}). \quad (\text{A2})$$

So, for $j = 1, \dots, n$, we obtain

$$\frac{\partial C_L^{(j)}}{\partial t} = - \left\{ \frac{\left(1 - k_0^{(j)} \right) C_L^{(j)} \frac{\partial g_L}{\partial t} + g_L (1 - \beta) \mathbf{v}_L \cdot \nabla C_L^{(j)}}{g_L (1 - \beta) + (1 - g_L) \gamma^{(j)} k_0^{(j)}} \right\}, \quad (\text{A3})$$

which already differs from Eq. (2) in [9] when $\gamma^{(j)} \neq 0$. Rearranging (A3) to the form

$$\left(\frac{1 - k_0^{(j)}}{1 - \beta} \right) \frac{C_L^{(j)}}{g_L} \frac{\partial g_L}{\partial t} = - \left(1 + \frac{\gamma^{(j)}}{g_L} \left(\frac{1 - g_L}{1 - \beta} \right) k_0^{(j)} \right) \frac{\partial C_L^{(j)}}{\partial t} - \mathbf{v}_L \cdot \nabla C_L^{(j)}, \quad (\text{A4})$$

and noting that

$$\frac{\partial T}{\partial t} = \sum_{j=1}^n f'(C_L^{(j)}) \frac{\partial C_L^{(j)}}{\partial t}, \quad \nabla T = \sum_{j=1}^n f'(C_L) \nabla C_L^{(j)}, \quad (\text{A5})$$

multiplication of (A4) by $f'(C_L^{(j)})$ and summation over j leads to

$$\frac{1}{g_L} \left\{ \sum_{j=1}^n f'(C_L^{(j)}) \left(\frac{1 - k_0^{(j)}}{1 - \beta} \right) C_L^{(j)} \right\} \frac{\partial g_L}{\partial t} = - \sum_{j=1}^n \left(1 + \frac{\gamma^{(j)}}{g_L} \left(\frac{1 - g_L}{1 - \beta} \right) k_0^{(j)} \right) f'(C_L^{(j)}) \frac{\partial C_L^{(j)}}{\partial t} - \sum_{j=1}^n f'(C_L) \mathbf{v}_L \cdot \nabla C_L^{(j)}, \quad (\text{A6})$$

which can also be rewritten as

$$\left\{ \sum_{j=1}^n f'(C_L^{(j)}) \left(1 - k_0^{(j)} \right) C_L^{(j)} \right\} \frac{\partial g_L}{\partial t} = - (1 - \beta) g_L \frac{DT}{Dt} - (1 - g_L) \sum_{j=1}^n \gamma^{(j)} k_0^{(j)} f'(C_L^{(j)}) \frac{\partial C_L^{(j)}}{\partial t}. \quad (\text{A7})$$

For a binary alloy, i.e. $n = 1$, we recover Eq. (29). As regards remelting, since $f'(C_L^{(j)}) < 0$ and $k_0^{(j)}, \beta < 1$, the condition that $\partial g_L / \partial t > 0$ implies that

$$(1 - \beta) g_L \frac{DT}{Dt} + (1 - g_L) \sum_{j=1}^n \gamma^{(j)} k_0^{(j)} f'(C_L^{(j)}) \frac{\partial C_L^{(j)}}{\partial t} > 0, \quad (\text{A8})$$

which reduces to (3) if $\gamma^{(j)} k_0^{(j)} = 0$ for $j = 1, \dots, n$.

Finally, combining the analysis in this appendix with that in Section 5 for the case of continuous casting, we have Eq. (57) and, for $j = 1, \dots, n$,

$$(1 - \beta) \frac{\partial}{\partial t} \left(g_L C_L^{(j)} \right) - k_0^{(j)} C_L \frac{\partial g_L}{\partial t} + \gamma^{(j)} (1 - g_L) k_0^{(j)} \frac{\partial C_L^{(j)}}{\partial t} + (1 - \beta) \nabla \cdot \left(g_L C_L^{(j)} \mathbf{v}_L \right) + k_0^{(j)} V_{\text{cast}} \left[\gamma^{(j)} (1 - g_L) \frac{\partial C_L^{(j)}}{\partial z} - C_L^{(j)} \frac{\partial g_L}{\partial z} \right] = 0, \quad (\text{A9})$$

which will lead to

$$\left(1 - k_0^{(j)} \right) C_L^{(j)} \frac{Dg_L}{Dt} = - (1 - \beta) g_L \frac{DC_L^{(j)}}{Dt} - \gamma^{(j)} (1 - g_L) k_0^{(j)} \frac{DC_L^{(j)}}{Dt}. \quad (\text{A10})$$

Multiplication of (A4) by $f'(C_L^{(j)})$ and summation over j leads to

$$\left[\sum_{j=1}^n \left(1 - k_0^{(j)} \right) f'(C_L^{(j)}) C_L^{(j)} \right] \frac{Dg_L}{Dt} = - (1 - \beta) g_L \frac{DT}{Dt} - (1 - g_L) \sum_{j=1}^n \gamma^{(j)} k_0^{(j)} f'(C_L^{(j)}) \frac{DC_L^{(j)}}{Dt}. \quad (\text{A11})$$

Then, for remelting, we require $\partial g_L / \partial t > 0$, which leads to

$$(1 - \beta) g_L \frac{DT}{Dt} + (1 - g_L) \sum_{j=1}^n \gamma^{(j)} k_0^{(j)} f'(C_L^{(j)}) \frac{DC_L^{(j)}}{Dt} > - \left[\sum_{j=1}^n \left(1 - k_0^{(j)} \right) f'(C_L^{(j)}) C_L^{(j)} \right] V_{\text{cast}} \frac{\partial g_L}{\partial z} \quad (\text{A12})$$

and reduces to (A8) when $V_{\text{cast}} = 0$.

References

- [1] E.J. Pickering, Macrosegregation in steel ingots: the applicability of modelling and characterisation techniques, *ISIJ Int.* 53 (2013) 935–949.
- [2] M.C. Flemings, G.E. Nereo, Macrosegregation. I, *Trans. TMS-AIME* 239 (1967) 1449–1461.
- [3] M.C. Flemings, *Solidification Processing*, McGraw-Hill, New York, 1974.
- [4] R. Mehrabian, M. Keane, M.C. Flemings, Interdendritic fluid flow and macrosegregation; influence of gravity, *Metall. Trans.* 1 (1970) 1209–1220.
- [5] J.J. Moore, N.A. Shah, Mechanisms of formation of A- and V-segregation in cast steel, *Int. Met. Rev.* 28 (1983) 338–384.
- [6] J. Li, M. Wu, J. Hao, A. Kharicha, A. Ludwig, Simulation of channel segregation using a two-phase columnar solidification model - Part II: mechanism and parameter study, *Comput. Mater. Sci.* 55 (2012) 419–429.
- [7] V.R. Voller, J.J. Moore, N.A. Shah, Modification of mathematical analyses and related physical descriptions used to describe channel segregation, *Metals Technol.* 10 (1983) 81–84.
- [8] R. Mehrabian, M.C. Flemings, Macrosegregation in ternary alloys, *Metall. Trans.* 1 (1970) 455–464.
- [9] T. Fujii, D.R. Poirier, M.C. Flemings, Macrosegregation in a multicomponent low-alloy steel, *Metall. Trans. B* 10 (1979) 331–339.
- [10] P. Auburtin, T. Wang, S.L. Cockcroft, A. Mitchell, Freckle formation and freckle criterion in superalloy castings, *Metall. Mater. Trans. B* 31 (2000) 801–811.
- [11] H. Tomono, Y. Hitomi, S. Ura, A. Teraguchi, K. Iwata, K. Yasumoto, Mechanism of formation of the V-shaped segregation in the large section continuous cast bloom, *Trans. ISIJ* 24 (1984) 917–922.
- [12] T. Brune, K. Kortzak, D. Senk, N. Reuther, M. Schaeperkoetter, A three dimensional model to characterize the centerline segregation in CC slabs, *Steel Res. Intl.* 86 (2015) 33–39.
- [13] T.B. Abbott, I.B. Hoyle, A.S. Woodyatt, The 3-dimensional structure of macrosegregation in continuously cast high-carbon steel, *Steel Res.* 65 (1994) 128–131.
- [14] X. Ma, D. Li, Characterization, mechanism and control measures of V segregation in continuous casting billet of C-Mn steel, *Metall. Mater. Trans. B* 50 (2019) 1161–1170.
- [15] R. Guan, C. Ji, M. Zhu, S. Deng, Numerical simulation of V-shaped segregation in continuous casting blooms based on a microsegregation model, *Metall. Mater. Trans. B* 49 (2018) 2571–2583.
- [16] K. Suzuki, T. Miyamoto, On the formation mechanism of V segregation in steel ingot, *Trans. ISIJ* 14 (1974) 296–305.
- [17] A.C. Fowler, The formation of freckles in binary-alloys, *IMA J. Appl. Maths.* 35 (1985) 159–174.
- [18] M.G. Worster, Convection in mushy layers, *Annu. Rev. Fluid Mech.* 29 (1997) 91–122.
- [19] P.W. Emms, A.C. Fowler, Compositional convection in the solidification of binary-alloys, *J. Fluid Mech.* 262 (1994) 111–139.
- [20] A. Plotkowski, M.J.M. Krane, On the numerical prediction of channel segregation, *Int. J. Heat Mass Transf.* 100 (2016) 11–23.
- [21] I. Vušanovic, V.R. Voller, Best practice for measuring grid convergence in numerical models of alloy solidification, *Int. J. Num. Meth. Heat Fluid Flow* 26 (2016) 427–439.
- [22] I. Vušanovic, V.R. Voller, Understanding channel segregates in numerical models of alloy solidification: a case of converge first ask questions later, *Mater. Sci.* 790–791 (2014) 74–78.
- [23] S.D. Felicelli, J.C. Heinrich, D.R. Poirier, Simulation of freckles during vertical solidification of binary-alloys, *Metall. Trans. B* 22 (1991) 847–859.
- [24] P.W. Emms, Freckle formation in a solidifying binary alloy, *J. Eng. Maths* 33 (1998) 175–200.
- [25] J. Ni, C. Beckermann, A volume-averaged two-phase model for transport phenomena during solidification, *Metall. Mater. Trans. B* 22B (1991) 349–361.
- [26] C.R. Swaminathan, V.R. Voller, Towards a general numerical scheme for solidification systems, *Int. J. Heat Mass Transf.* 40 (1997) 2859–2868.
- [27] M. Vynnycky, S. Saleem, H. Fredriksson, An asymptotic approach to solidification shrinkage-induced macrosegregation in the continuous casting of binary alloys, *Appl. Math. Mod.* 54 (2018) 605–626.
- [28] M. Vynnycky, On the formation of centreline shrinkage porosity in the continuous casting of steel, *J. Math. Industry* 10 (2020). Article no. 14 (26 pages)
- [29] M. Assunção, M. Vynnycky, S.L. Mitchell, On small-time similarity-solution behaviour in the solidification shrinkage of binary alloys, *Eur. J. Appl. Maths* 32 (2021) 199–225.
- [30] T.W. Clyne, W. Kurz, Solute redistribution during solidification with rapid solid-state diffusion, *Met. Trans.* A 12 (1981) 965–971.
- [31] H.B. Brody, M.C. Flemings, Solute redistribution in dendritic solidification, *Trans. AIME* 236 (1966) 615–624.
- [32] J.C. Heinrich, D.R. Poirier, Convection modeling in directional solidification, *C. R. Mecanique* 332 (2004) 429–445.
- [33] M. Rappaz, V. Voller, Modeling of micro-macro-segregation in solidification processes, *Metall. Trans. A* 21 (1990) 749–753.
- [34] A. Kumar, P. Dutta, S. Sundarraj, M.J. Walker, Remelting of solid and its effect on macrosegregation during solidification, *Numer. Heat Transf. A* 51 (2007) 59–83.
- [35] A.O.P. Chiareli, M.G. Worster, On measurement and prediction of the solid fraction within mushy layers, *J. Crystal Growth* 125 (1992) 487–494.
- [36] V.R. Voller, A.D. Brent, C. Prakash, The modeling of heat, mass and solute transport in solidification systems, *Int. J. Heat Mass Transf.* 32 (1989) 1719–1731.
- [37] V.R. Voller, A.D. Brent, C. Prakash, Modeling the mushy region in a binary alloy, *Appl. Math. Mod.* 14 (1990) 320–326.
- [38] I. Vusanovic, V.R. Voller, Reduced complexity solidification models, *Int. J. Heat Mass Transf.* 169 (2021). Article no. 120923 (11 pages)
- [39] C.J. Vreeman, F.P. Incropera, The effect of free-floating dendrites and convection on macrosegregation in direct chill cast aluminum alloys. Part II: predictions for Al-Cu and Al-Mg alloys, *Int. J. Heat Mass Transf.* 43 (2000) 687–704.
- [40] B.C.H. Venneker, L. Katgerman, Modelling issues in macrosegregation predictions in direct chill castings, *J. Light Met.* 2 (2002) 149–159.
- [41] M. Založnik, S. Xin, B. Šarler, Verification of a numerical model of macrosegregation in direct chill casting, *Int. J. Num. Meth. Heat Fluid Flow* 18 (2008) 308–324.
- [42] Q. Du, D.G. Eskin, L. Katgerman, Modeling macrosegregation during direct-chill casting of multicomponent aluminum alloys, *Metall. Mater. Trans. A* 38A (2007) 180–189.
- [43] Q. Du, D.G. Eskin, L. Katgerman, Numerical issues in modelling macrosegregation during DC casting of a multi-component aluminium alloy, *Int. J. Num. Meth. Heat Fluid Flow* 19 (2009) 917–930.
- [44] T. Jalanti, M. Swierkosz, M. Gremaud, M. Rappaz, Modelling of macrosegregation in continuous casting of aluminium, in: K. Ehrke, W. Schneider (Eds.), *Continuous Casting*, WILEY-VCH Verlag GmbH, Weinheim, 2006, pp. 191–198.
- [45] E.J. Pickering, S.S. Al-Bermani, J. Talamantes-Silva, Application of criterion for A-segregation in steel ingots, *Mater. Sci. Tech.* 31 (2015) 1313–1319.
- [46] M.T. Rad, P. Kotas, C. Beckermann, Rayleigh number criterion for formation of A-segregates in steel castings and ingots, *Metall. Mater. Trans. A* 44A (9) (2013) 4266–4281.
- [47] C. Beckermann, J.P. Gu, W.J. Boettinger, Development of a freckle predictor via Rayleigh number method for single-crystal nickel-base superalloy castings, *Metall. Mater. Trans. A* 31 (2000) 2545–2557.
- [48] W.H. Yang, W. Chen, K.M. Chang, S. Mannan, J. deBarbado, Freckle criteria for the upward directional solidification of alloys, *Metall. Mater. Trans. A* 32 (2001) 397–406.